



**HAL**  
open science

## Ocean variability over the Agulhas Bank and its dynamical connection with the southern Benguela upwelling system.

Bruno Blanke, Pierrick Penven, Claude Roy, Nicolette Chang, Florian Kokoszka

### ► To cite this version:

Bruno Blanke, Pierrick Penven, Claude Roy, Nicolette Chang, Florian Kokoszka. Ocean variability over the Agulhas Bank and its dynamical connection with the southern Benguela upwelling system.. Journal of Geophysical Research. Oceans, 2009, 114, pp.C12028. 10.1029/2009JC005358 . hal-00453434

**HAL Id: hal-00453434**

**<https://hal.science/hal-00453434v1>**

Submitted on 13 Jan 2022

**HAL** is a multi-disciplinary open access archive for the deposit and dissemination of scientific research documents, whether they are published or not. The documents may come from teaching and research institutions in France or abroad, or from public or private research centers.

L'archive ouverte pluridisciplinaire **HAL**, est destinée au dépôt et à la diffusion de documents scientifiques de niveau recherche, publiés ou non, émanant des établissements d'enseignement et de recherche français ou étrangers, des laboratoires publics ou privés.

Copyright

## Ocean variability over the Agulhas Bank and its dynamical connection with the southern Benguela upwelling system

Bruno Blanke,<sup>1</sup> Pierrick Penven,<sup>2,3</sup> Claude Roy,<sup>2</sup> Nicolette Chang,<sup>3,4</sup> and Florian Kokoszka<sup>2</sup>

Received 12 February 2009; revised 23 September 2009; accepted 25 September 2009; published 30 December 2009.

[1] This study analyzes the oceanic pathway connecting the Agulhas Bank to the southern Benguela upwelling system by means of a quantitative Lagrangian interpretation of the velocity field calculated by a high-resolution numerical simulation of the ocean around the southwestern tip of Africa. The regional ocean model is forced with National Centers for Environmental Prediction surface winds over 1993–2006 and offers a relevant numerical platform for the investigation of the variability of the water transferred between both regions, both on seasonal and intraseasonal time scales. We show that the intensity of the connection fluctuates in response to seasonal wind variability in the west coast upwelling system, whereas intraseasonal anomalies are mostly related to the organization of the eddy field along the southwestern edge of the Agulhas Bank. Though the study only considers passive advection processes, it may provide useful clues about the strategy adopted by anchovies in their selection of successful spawning location and period. The pathway under investigation is of major interest for the ecology of the southern Benguela upwelling system because it connects the spawning grounds on the Agulhas Bank with the nursery grounds located on the productive upwelling off the west coast.

**Citation:** Blanke, B., P. Penven, C. Roy, N. Chang, and F. Kokoszka (2009), Ocean variability over the Agulhas Bank and its dynamical connection with the southern Benguela upwelling system, *J. Geophys. Res.*, 114, C12028, doi:10.1029/2009JC005358.

### 1. Introduction

[2] The Agulhas Bank forms the southern limit of the Benguela upwelling system (see Figure 1). It extends from off Cape Peninsula around 18°E to Port Alfred at about 26°E. Its meridional extent encompasses the full continental shelf within 34°S–37°S and with depths shallower than 200 m. The Agulhas Current flows along its southeastern edge. This current originates much further north in the Indian Ocean along the eastern coast of Africa and it retroflects southwest of the Agulhas Bank, giving birth to an intense eddy activity made of meanders, eddies and filaments. These mesoscale features move northwestward and can interact with the dynamics of the southern Benguela upwelling system. Westerly winds are dominant over the Agulhas Bank but transient easterly episodes, especially in summer and fall, can generate local upwelling cells [Hardman-Mountford *et al.*, 2003; Shillington *et al.*, 2006]. However, most upwelling phenomena (like the Port Alfred upwelling cell) are related to interaction of the Agulhas

Current with the continental slope on the edge of the Agulhas Bank [Lutjeharms *et al.*, 1989]. By comparison, the Benguela upwelling system is much more intense and steadier. It is located on the west and southwest coast of southern Africa. The dynamics of the upwelling is driven by prevailing equatorward winds that induce an intense off-shore Ekman transport. In the southern Benguela region, the variability of the upwelling mostly concentrates around a few upwelling cells: the Namaqua cell around 30°S, the Cape Columbine cell around 32.5°S and the Cape Peninsula cell around 34°S [Weeks *et al.*, 2006]. Subsurface waters upwell all yearlong but the winds are most intense from October to February, leading to accentuated sea surface temperature (SST) contrasts between the open ocean and the inner shelf during summer.

[3] The Agulhas Bank is a major spawning ground for anchovies whose eggs and larvae are transported afterward, particularly via the Good Hope Jet that flows along the shelf edge off the Cape Peninsula [Bang and Andrews, 1974], toward the southwestern coast of Africa where they mature, within the nutrient-rich waters of the southern Benguela upwelling system [Shelton and Hutchings, 1982; Hutchings, 1992]. A few months later, young anchovy recruits migrate back to the Agulhas Bank where they can represent a significant portion of the adult spawning population. The southern portion of the Benguela upwelling system that is relevant to our study extends from 32°S to 35°S and is mostly made of Saint Helena Bay, which is the major nursery ground along the west coast, and the ocean from

<sup>1</sup>Laboratoire de Physique des Océans, UMR 6523, UBO, CNRS, IRD, IFREMER, Brest, France.

<sup>2</sup>Laboratoire de Physique des Océans, UMR 6523, UBO, IRD, CNRS, IFREMER, Plouzané, France.

<sup>3</sup>Department of Oceanography, UCT, Cape Town, South Africa.

<sup>4</sup>Center for High Performance Computing, CSIR, Cape Town, South Africa.

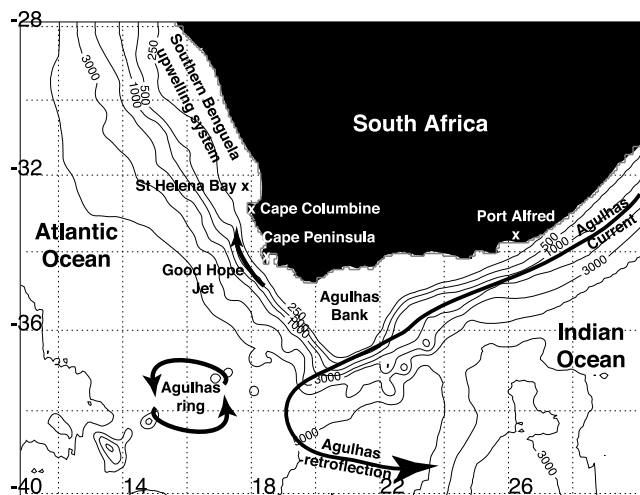


**Figure 1.** Model domain and localization of the main geographical places and dynamical features used in the text. Bathymetry contours 250, 500, 1000, 2000, 3000, 4000, and 5000 m are drawn with a thin line.

southwest of Cape Agulhas to Cape Columbine. This latter area is traveled northwestward by anchovy's eggs and larvae during their journey to the west coast, and southeastward by young adults on their way back to the Agulhas Bank spawning ground. The southern Benguela upwelling system includes a strong, surface-intensified, coastal jet related to the Benguela Current and a countercurrent that flows southward along the continental slope [Shillington *et al.*, 2006].

[4] This study aims at depicting and quantifying the progression of ocean waters from the Agulhas Bank to the southern Benguela upwelling system, making use of the velocity field simulated by a high-resolution ocean model forced with atmospheric fluxes that incorporate intraseasonal as well as seasonal and interannual variability. We put the stress on wind forcing since the seasonal and interannual variability of the Benguela upwelling system depends significantly on wind variability [Blanke *et al.*, 2002, 2005], with the appearance of subsequent SST anomalies along the coast and possible long-term spatial reorganization of the marine ecosystem [van der Lingen *et al.*, 2002]. We use the IRD (Institut de Recherche pour le Développement) version of the ROMS-UCLA, free surface, primitive equation ocean model [see Shchepetkin and McWilliams, 2005; Penven *et al.*, 2006a]. Particle trajectories calculated with the ARIANE algorithm [Blanke and Raynaud, 1997; Blanke *et al.*, 1999] are used to depict the advective transport of water from the Agulhas Bank to the southern Benguela upwelling system over 1993–2006, a period over which the model is forced with National Centers for Environmental Prediction (NCEP) atmospheric surface fluxes. Statistics about time scales and spatial organization are built from the initial and final positions of the particles on the Agulhas Bank and at the entrance of Saint Helena Bay, respectively. Section 2 of the paper presents the ocean model and the Lagrangian calculations. Section 3 introduces the mean statistics obtained over the full period of investigation. Seasonal variability and anomalies with respect to a

mean seasonal description are discussed in section 4, before a discussion and our conclusions are given in section 5.

## 2. Method

### 2.1. Ocean Model

[5] The parent model corresponds to the Southern Africa Experiment (SAfE) [Penven *et al.*, 2006a, 2006b]. This ROMS configuration was built using ROMSTOOLS (<http://roms.mpl.ird.fr/>) [Penven *et al.*, 2007] and is designed for the resolution of the major phenomena around southern Africa. The Mercator grid has an increment of  $0.25^\circ$ , ranging from  $2.5^\circ\text{W}$  to  $54.75^\circ\text{E}$  and from  $46.75^\circ$  to  $4.8^\circ\text{S}$ , and the horizontal resolution ranges from 19 km in the south to 27.6 km in the north. The vertical resolution is based on 32  $\sigma$  coordinate levels that are stretched toward the surface. A radiation scheme at the lateral boundaries connects the model with its surroundings, while inflow conditions are nudged toward data obtained from the WOA 2001 database [Conkright *et al.*, 2002].

[6] Then, a nested modeling approach was followed to model the Agulhas Bank and surroundings with a higher resolution without disregarding variability at larger scales. The two-way, grid-embedding capability of ROMS was employed, in which a sequence of structured grid models are able to interact with one another [Penven *et al.*, 2006c]. The embedding procedure makes use of the AGRIF (Adaptive Grid Refinement in Fortran) package [Blayo and Debreu, 1999]. The high-resolution child model is designed to encompass the Agulhas Bank and its surroundings and has a temporal and spatial resolution three times finer than the parent grid (approximately 15 min and 8 km, respectively). The child model has  $233 \times 185$  grid points in the horizontal plane, encompassing the area from  $11^\circ\text{E}$  to  $30^\circ\text{E}$  and from  $27.7^\circ$  to  $40.3^\circ\text{S}$ . The parent grid supplies the boundary conditions of the child grid. Both the parent and child models use the general bathymetric chart of the World Oceans (GEBCO) for the bottom topography and start from rest. They are forced at the surface with the 1948 to present NCEP reanalysis available with 6 hours in time and  $1.875^\circ$  in space resolution. The wind forcing is applied as a stress and the other surface fluxes are calculated with bulk formula derived from the Coupled Ocean/Atmosphere Mesoscale Prediction System [Hodur, 1997] without addition of any restoring term. This parent-child configuration was run from 1993 to 2006 after a 3 year spin-up to reach statistical equilibrium. Model outputs were averaged and stored every 2 days of simulation. The variance of the child model sea level is in fair agreement with that deduced from satellite observations of the absolute dynamic topography, i.e., sea surface elevation above the geoid height obtained from the sum of weekly sea level anomalies and the Rio05 mean dynamic topography [see Ducet *et al.*, 2000; Rio and Hernandez, 2004]. Time-mean energetics of the retroflection area of the Agulhas Current and of the region over the Agulhas Plateau (around  $27^\circ\text{E}$ ,  $40^\circ\text{S}$ ) show equivalent intensity (Figure 2), keeping in mind the difference in time and space resolution of both data sets. The variability of the sea level over the continental shelf of the southern Benguela upwelling system is also equivalent (Figure 3), knowing that internal variability, which is uncorrelated between model and genuine observations, adds to surface forcing

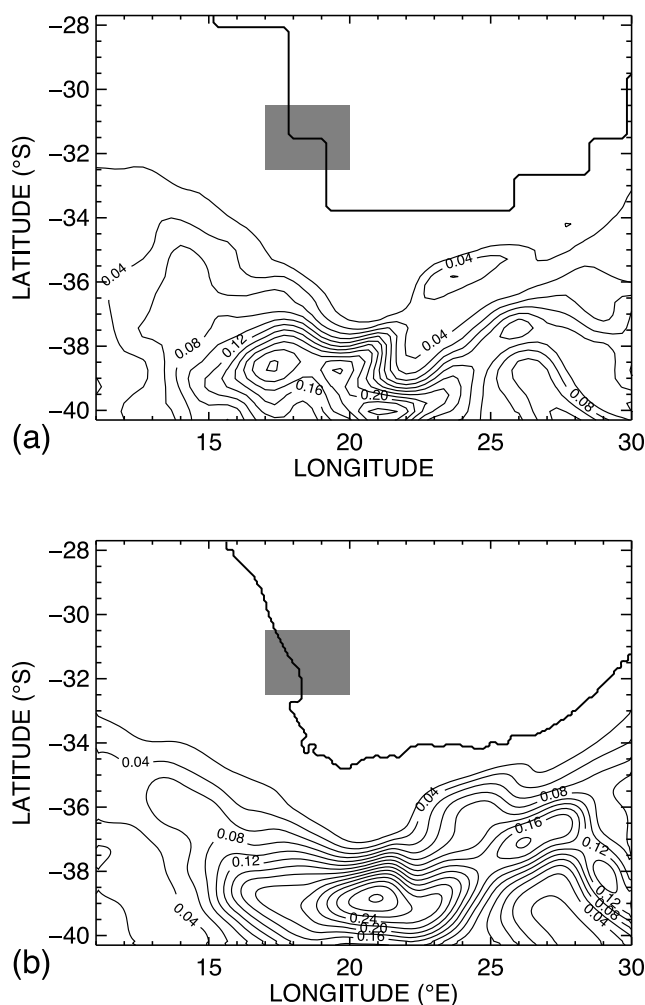


**Figure 2.** Variance of the surface sea level over 1993–2006 with a 0.01 m contour interval (a) for the observed dynamic topography and (b) for the model. The area in the southern Benguela upwelling system used to diagnose the time series shown in Figure 3 is shaded.

in generating upward and downward movements of the sea level at the coastline.

[7] In a configuration run with surface climatological forcing, the same model is able to reproduce the important features of the Agulhas Bank with, among other elements, the strong seasonality of the temperature structure, the effect of the Agulhas Current on the currents of the Agulhas Bank, and the cool tongue (Cool Ridge) on the East Agulhas Bank [Chang, 2009]. The fastest currents on the West Agulhas Bank are the coastal upwelling jet, the outer shelf current and the Good Hope Jet. The latter two show seasonal fluctuations with strongest currents in summer and weakest in winter. Flow on the Agulhas Bank east of 20.8°E is dominated by westward currents. Coastal flow is aligned with the coast. In winter, reverse eastward flow is found close to the coast. The mean currents increase in magnitude from the coast offshore. The strongest flow, on the outer shelf, is associated with the Agulhas Current. It has a tendency to move off the shelf repeatedly, whatever the season, while turbulent structures develop over the shelf. Currents along the coast and on the inner shelf flow more

easily westward onto the Western Agulhas Bank [Chang, 2009].

## 2.2. Lagrangian Calculations

[8] The off-line Lagrangian calculations are done with the ARIANE algorithm (<http://www.univ-brest.fr/lpo/ariane/>) [Blanke and Raynaud, 1997; Blanke et al., 1999]. The approach allows volume transport estimates on the basis of infinitesimal weights allotted to numerical particles and transported along their trajectories. Within this framework, numerical floats are used to reproduce the movement induced by the dynamics explicitly calculated by the ocean model without mimicking the behavior of true individual water parcels that would be of course aware of both advection and subgrid-scale diffusion phenomena. The approach allows interpretation of temperature and salinity variations along a trajectory as the integrated effect of direct warming by the solar heat flux, runoff, precipitation and evaporation processes, and mean lateral and vertical turbulent diffusion in the ocean model, i.e., water mass transformation [Blanke et al., 1999].

[9] The connection from the Agulhas Bank to the southern Benguela upwelling system is here computed with millions of numerical particles released along a meridional section across the Agulhas Bank at 20.8°E (south of Cape Agulhas) and over the shelf and the slope shallower than 1200 m (i.e., north of 37°S). Initial positions for particles are spread over the successive time steps of the model archived velocity field, using a distribution technique derived from Blanke and Raynaud [1997]. The maximum transport carried by each particle is chosen equal to  $T_0 = 100 \text{ m}^3/\text{s}$  per 2 day period, so that individual model grid cells (on the 20.8°E section) may see their transport,  $T_i$ , described by more than one (namely  $N_i$ ) particle, with  $N_i$  satisfying  $T_i/(N_i)^3 \leq T_0$ . If  $N_i$  is 1, the particle is positioned right at the center of the model grid cell and will start moving from the middle of the time interval under consideration. For greater values of  $N_i$ , the  $(N_i)^3$  initial positions are regularly distributed both in space (along the vertical and meridional extent of the grid cell) and in time (still within the same 2 day interval). Each particle is allotted a weight equal to a fraction of the local westward flow so that the sum of all weights amounts to the full magnitude of the westward transport. Particles initialized within the same grid cell are of course allotted the same weight, i.e.,  $T_i/(N_i)^3$ . Trajectories (with related infinitesimal transports) are integrated forward in time till they reach specific final sections (see Figure 4). These vertical sections completely close the area of interest from 12.7 to 20.8°E and 30.45 to 37.5°S. Some special care was taken to define the interception section located within the Benguela upwelling system: this section follows at best the 200 m isobath in order to stop trajectories when they do reach the continental shelf. Each trajectory is computed offline and integrated sequentially on the 2 day mean fields of the simulation for 1 year at most, in order to limit the burden of the computations and to give each particle a same maximum lifetime to connect the initial section at 20.8°E to another control section. The numerical particles are released starting from year 1993 of the simulation. We stop the deployment at the end of year 2005 allowing to the last released particles a 1 year delay to exit the domain. At the end of the integration, only a very small

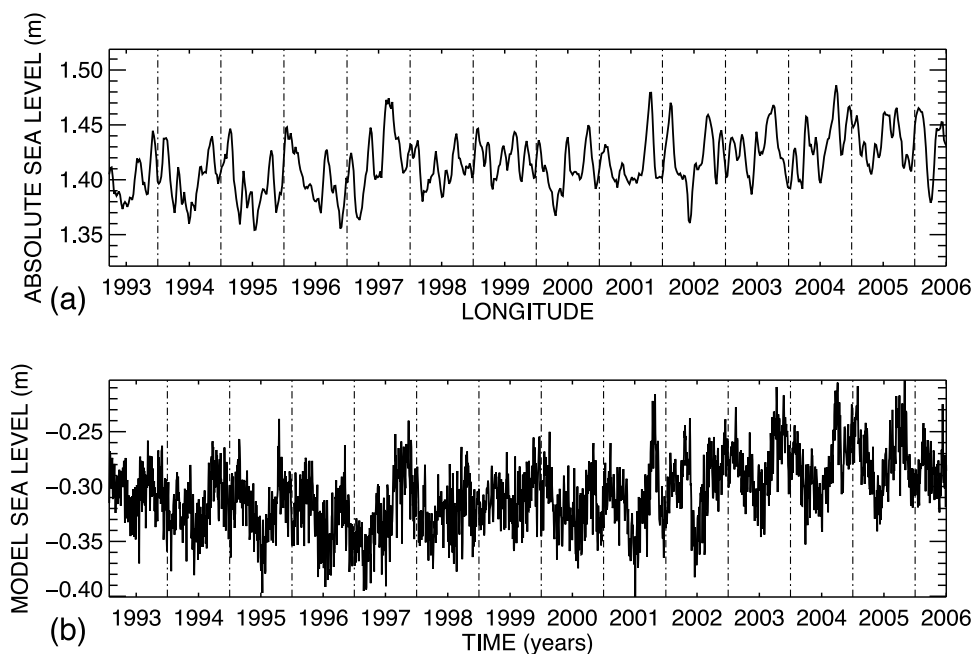


**Figure 3.** Time series of the surface sea level averaged over the area  $[17.0^{\circ}\text{E}–18.5^{\circ}\text{E}] \times [32.5^{\circ}\text{S}–30.5^{\circ}\text{S}]$  (a) for the observed dynamic topography and (b) for the model. Note that the observations and the model differ about their zero reference level.

percentage of particles are still in the domain (and explain less than 0.4% of the total incoming transport): such particles could not connect the initial section to another geographical section in less than 1 year. The average water mass transfer between the Agulhas Bank at  $20.8^{\circ}\text{E}$  and the southern Benguela shelf thus derived is  $0.38\text{ Sv}$  ( $1\text{ sverdrup} = 10^6\text{ m}^3/\text{s}$ ); it is simply obtained by summing the weight of all the particles that participate in the transfer. All the Lagrangian computations can be done in two different ways, as explained by *Blanke and Raynaud* [1997]. Off-line diagnostics allow backward computations of trajectories (simply by multiplying all velocity outputs by  $-1$ , and reversing their order). The joint use of backward and forward Lagrangian calculations thus gives access to a measurement of the error made in computing directional transports, as any transport (from section A to section B) can be calculated in two independent ways: in-seminating A and summing the transports of the particles that do reach B, or in-seminating B and summing the transports of the particles that do originate from A. The size of the resulting error is of the order of the infinitesimal transport given to each individual particle. The number of particles we use in this study would allow us to define Lagrangian transports with accuracy better than  $0.002\text{ Sv}$ , assuming that all particles can be tracked in time till they are intercepted at control sections. Though the estimation of the Lagrangian transports is quite robust, the limitation put on the time of integration (1 year) leads to additional uncertainty on the fate of a small fraction of the full westward flow at  $20.8^{\circ}\text{E}$ . Therefore, we put a reasonable estimate of the error on the computed mean transports at  $0.01\text{ Sv}$ . This accuracy was verified with the outcome of a twin reverse experiment in which initial particles were deployed over the edge of the southern Benguela shelf over 1994–2006 and integrated

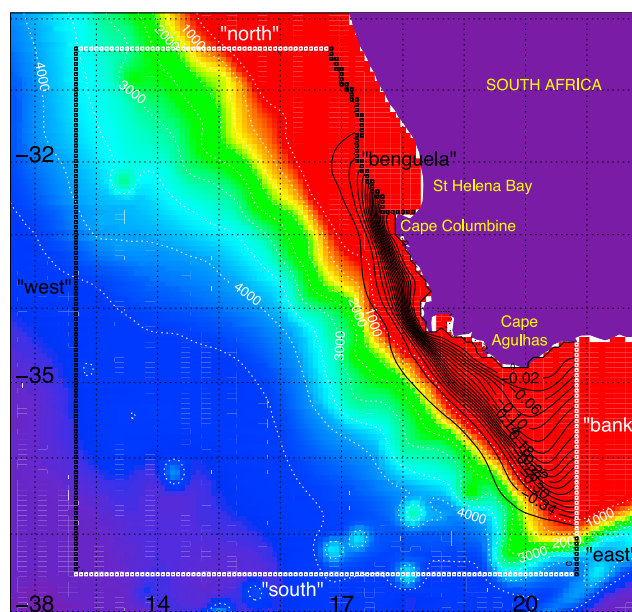


**Figure 4.** In black, Lagrangian stream function for the mass transfer from the Agulhas Bank to the southern Benguela upwelling system. The contour interval is  $0.02\text{ Sv}$ . The domain of calculation of the stream function is bounded by six interception sections:  $20.8^{\circ}\text{E}$  from the coastline to  $37^{\circ}\text{S}$  (“bank”),  $20.8^{\circ}\text{E}$  from  $37^{\circ}\text{S}$  to  $37.5^{\circ}\text{S}$  (“east”),  $37.5^{\circ}\text{S}$  (south),  $12.7^{\circ}\text{E}$  (west),  $30.45^{\circ}\text{S}$  (north), and the edge of the southern Benguela shelf (“benguela”). The model bathymetry is shaded in color together with white dotted lines with a  $500\text{ m}$  contour interval. Yellow labels identify specific geographical places introduced in the text.

**Table 1.** Mean Statistics and Related Standard Deviation at 20.8°E for Latitude, Depth, Salinity, and Temperature for the Various Possible Transfers Achieved by the Waters Initially on the Agulhas Bank<sup>a</sup>

Interception Section	Flow (Sv)	Latitude (°)		Depth (m)		Salinity (psu)		Temperature (°C)	
		Mean	SD	Mean	SD	Mean	SD	Mean	SD
Bank	0.41	-36.40	0.76	-248.8	262.2	34.99	0.22	12.4	4.5
East	0.09	-36.93	0.16	-573.0	364.8	34.83	0.20	8.8	4.9
South	1.97	-36.86	0.23	-228.5	212.4	35.08	0.20	14.7	4.6
West	0.79	-36.47	0.61	-129.3	149.9	35.10	0.17	15.3	3.7
North	0.35	-36.20	0.73	-78.6	82.6	35.13	0.11	15.9	2.7
Benguela	0.38	-35.84	0.75	-75.9	71.2	35.13	0.11	14.8	2.4

<sup>a</sup>SD, standard deviation. Eventual transmissions of water are toward one of the six interception sections under consideration (see Figure 4). The results obtained for latitude and depth are shown in Figure 5 on a meridional section across the Agulhas Bank. The statistics are calculated from the physical properties attached to each set of Lagrangian particles.

backward in time for a maximum of 1 year so that their origin could be assessed along the edge of the area of study.

### 3. Mean Integrated Vision

[10] The average forward transfer of 0.38 Sv is shown in Figure 4 as a stream function once particle individual movements are time and depth integrated [Blanke *et al.*, 1999]. The shelf nature of the connection stands out with very little transfer exported beyond the 500 m isobath. The flow on the Agulhas Bank is rather uniformly distributed whereas the access to the southern Benguela shelf is restricted to the southernmost fraction of the interception section. Other destinations for the flow initially considered on the Agulhas Bank are the initial section itself (for moments and locations where the velocity is eastward), the Indian Ocean at 20.8°E (south of 37°S), the Southern Ocean at 37°S, the South Atlantic Ocean at 12.7°E and the subtropical Atlantic Ocean at 30.45°S, with corresponding average volume transfers of 0.41, 0.09, 1.97, 0.79 and 0.35 Sv respectfully (see Table 1).

[11] The dominance of the southward export is explained by the extension of the initial section over the continental

slope, above depths that can reach 1200 m. There, initial particles account for a significant amount of Agulhas Current waters that are likely to retroflect toward the Indian Ocean without entering the Atlantic Ocean. Median initial positions on latitude versus depth and salinity versus temperature diagrams are given in Table 1, together with related standard deviations. One may easily check on Figure 5 that the fraction of the westward flow above the Agulhas Bank that reaches eventually the southern Benguela shelf is located on average on the inner shelf. Particles initiated at the vertical of the continental slope are more likely to be transported toward the Southern Ocean or back to the Indian Ocean. Waters with other destinations (“south,” “west,” and “north”) approximately lay out in tiers in that order on the Agulhas Bank, from the open ocean to the coast. On the Agulhas Bank, the tracer characteristics of the waters transmitted to the southern Benguela shelf have mean temperature and salinity of 14.8°C and 35.13 practical salinity unit (psu), respectively. They do not differ much from the waters transmitted elsewhere, except for those that recirculate to the Indian Ocean and that are associated with colder and fresher properties (8.9°C and 34.83 psu, respectively).

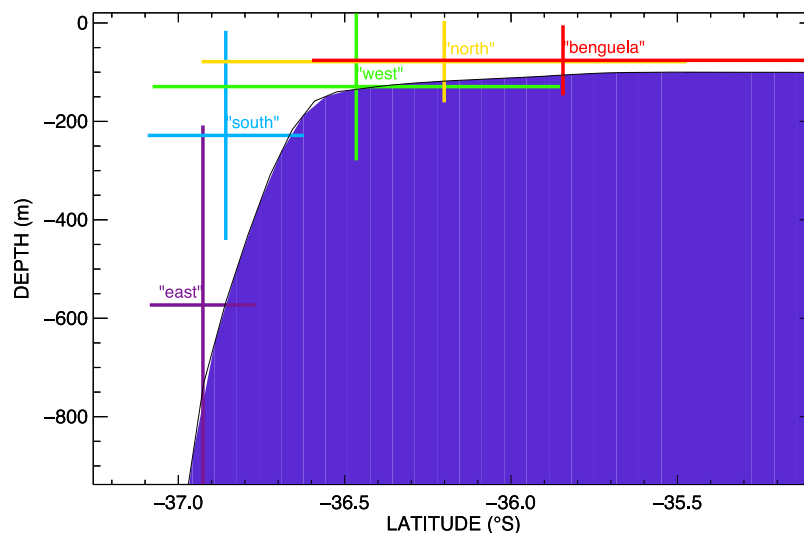


**Figure 5.** Mean statistics (cross center) and related standard deviation (cross extent) at 20.8°E on a latitude-depth diagram for the various possible transfers achieved by the waters initially on the Agulhas Bank (see Table 1). Each cross corresponds to transmission of water toward one of the five remote interception sections under consideration (every section except the Agulhas Bank itself, see Figure 4).

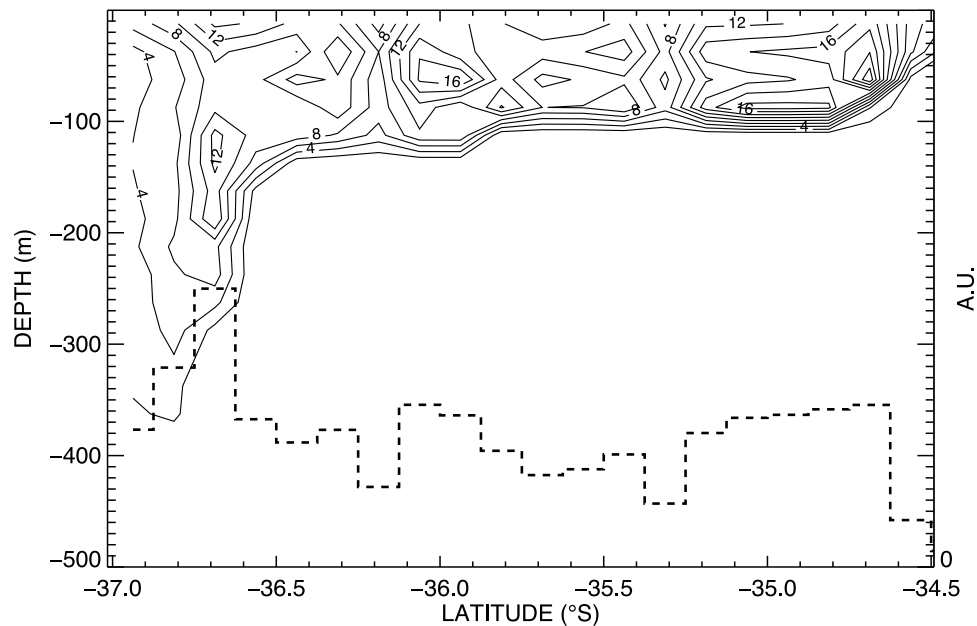


**Figure 6.** Remapping at  $20.8^{\circ}\text{E}$  of the transport explained by the particles that explain the mass transfer from the Agulhas Bank to the southern Benguela shelf. The contour interval is 2 mm/s. The histogram of the transport as a function of latitude, over  $0.125^{\circ}$  bands, is superimposed at the bottom as a thick dashed line with an arbitrary unit.

[12] Henceforth, we focus only on the particles that describe the water transfer to the southern Benguela shelf. The places on the initial section most favorable to an export to the west coast upwelling system are diagnosed by mapping on a regular grid at  $20.8^{\circ}\text{E}$ , with a  $0.125^{\circ} \times 25$  m spacing, the transport carried by the particles that do achieve this connection. The result is scaled by the area of each grid element to express it as a velocity (Figure 6). The flow is rather regularly distributed with latitude, although with a local maximum at the shelf edge and with depth over the first 100 m (with the exception of a deeper vein at 150 m, again at the shelf edge). It is worth noting that the distribution with depth favors subsurface layers. The transfer flowing at  $20.8^{\circ}\text{E}$  in the 25–50 m range is 20% larger than the transfer in the surface layer (0–25 m). This feature will be taken up in section 4.1 when discussing the effect of the surface wind stress along the journey from the Agulhas Bank to the west coast: surface waters are more likely driven away from the coast than subsurface waters during southeasterly wind episodes, and have less chances of reaching the upwelling system. In terms of relative intensity, we find that the transport transmitted to the southern Benguela shelf and initially in the surface layer (0–25 m) explains only 12.4% of the total available westward flow on the Agulhas Bank. The proportion increases to 17.6% for the water flowing in the 50–75 m range and it decreases to less than 7% for all depth ranges deeper than 100 m. An equivalent kind of transfer relative efficiency can be calculated with respect to the initial latitude band considered on the Agulhas Bank (Figure 7). The largest relative efficiency, 40.3%, is found near  $35^{\circ}\text{S}$ , i.e., midway between the coast and the middle of the continental shelf. It falls to 25% at the coast and to 20% at the shelf edge and much less beyond

(where the total available westward flow is however the largest, on account of the Agulhas Current).

## 4. Time Variability

### 4.1. Seasonal Scales

[13] The relative efficiency of the connection of the westward flow on the Agulhas Bank to the southern Benguela upwelling system is not frozen in time but varies on a seasonal scale, even though the largest efficiency always occurs on the internal shelf (between  $34.5$  and  $35.5^{\circ}\text{S}$  on Figure 7). It can reach more than 70% in the neighborhood of the coast in late winter (for an average efficiency over the whole shelf of about 40%) but it is much less during summer (15% on average over the whole shelf, with a maximum of only 25% near the coast). These fluctuations are worth investigating, by focusing on the initial and final temporal positions of the particles that explain the connection.

[14] We scale the final ages of particles into 1 day bins (see Figure 8) to derive useful properties such as the median time of the transfer, 58 days, or the times by which 10% and 90% of the transfer are achieved (32 and 120 days, respectively). Ten and ninety percents of the transfer are achieved within 1 and 3 months, respectively, and the fastest particle makes the connection in only 11.5 days. The mode of the distribution, i.e., the most frequent value for the connection time, is obtained for about 40 days, which is compatible with the anchovy life cycle patterns [Huggett *et al.*, 2003]. This happens to be the same value as the lag that maximizes the cross-correlation coefficient (0.74) of both time series of the transfer, when considered at  $20.8^{\circ}\text{E}$  and on the edge of the southern Benguela upwelling system (hereafter “inflow” and “outflow” time series, respectively).

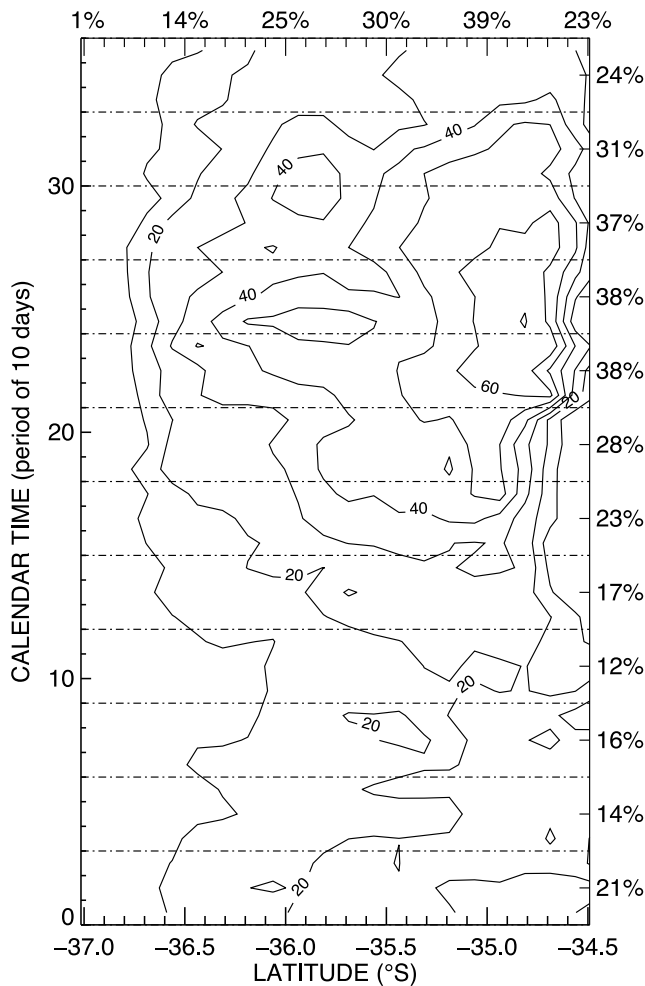


**Figure 7.** Seasonal relative efficiency of the transfer from the Agulhas Bank to the southern Benguela upwelling system with respect to the full available westward flow on the Agulhas Bank at  $20.8^{\circ}\text{E}$ , as a function of latitude and time, with a  $10\%$  contour interval. Monthly averaged values over the shelf and annual mean values for specific latitudes are written on the right-hand side and top axes, respectively.

[15] The disparity in ages stems of course from differences in initial velocity on the Agulhas Bank (depending on depth, latitude and time of departure), but also from the distance to be covered (to connect varied initial and final positions on the Agulhas Bank and on the southern Benguela shelf, respectively) and from the complexity of the trajectories that may involve transport by and recirculation in mesoscale structures. Figure 9 shows examples of diversified behaviors, starting from approximately the same geographical model grid point on the Agulhas Bank ( $20.8^{\circ}\text{E}$ ,  $35^{\circ}\text{S}$ , at the sea surface) and at the same season (mid summer) but at different instants of the simulation, and leading to total travel times that vary from 24 days (i.e., a short connection time) to slightly more than 6 months. Most displacements are done along the shelf edge but excursions into the open ocean do occur, either to the southwest of the Agulhas Bank or west of the Benguela upwelling system. Cross-shore movements take place as eddying pathways, because of capture by coherent structures. The complexity

of the trajectories also involves upward and downward migration, even though the depth range covered here by the selected set of particles does not extend beyond  $[0-80\text{ m}]$  (not shown).

[16] The inflow and outflow time series are characterized by a dominant seasonal cycle (Figure 10). We obtain intensified and weakened flows on the Agulhas Bank in September and April, respectively. The time series for the transfer considered at the entry of the southern Benguela shelf shows equivalent extremes, but 1–2 months later because of the advection time needed to make the connection. The correlation of each time series with a mean seasonal cycle built from the average of 12 successive years gives linear coefficients equal to 0.61 and 0.79, for the inflow on the Agulhas Bank and the outflow in the upwelling system, respectively. These two large correlation coefficients, with a seasonal signal more apparent downstream than upstream, suggest that the transfer of water from the Agulhas Bank to the southern Benguela upwelling system is conditioned by ocean variability either on the west coast of southern Africa or along the journey from the Agulhas Bank to the west coast upwelling. The seasonal variability of the transfer is not linked explicitly to upstream ocean variability (along the southeastern coast of South Africa). Indeed, seasonal variability is not dominant in the time series of the full westward flow available on the Agulhas Bank at  $20.8^{\circ}\text{E}$ ; it appears only in the fraction of the flow that eventually connects to the west coast upwelling system. In fact, on the Agulhas Bank, the linear correlation coefficient between the time series of the full westward flow and its mean seasonal cycle falls to 0.23 (not shown). The seasonal phasing obtained on the Agulhas Bank for relative efficiency (Figure 7) and intensity of the transfer (Figure 10a) reinforces the analysis that the full incoming westward flow on the Agulhas Bank does not govern the variability of the transfer eventually achieved to the southern Benguela upwelling system.

[17] In order to support this assumption about the origin of seasonal variability in the transfer, we performed an additional Lagrangian experiment in which the interception sections at  $30.45^{\circ}\text{S}$  and along the southern Benguela shelf were replaced by a unique zonal section at  $33.2^{\circ}\text{S}$ , i.e., south of Cape Columbine. In this new experiment, we used the exact same ensemble of numerical particles as in the reference experiment (i.e., their same initial positions on the Agulhas Bank at  $20.8^{\circ}\text{E}$ ), but the trajectories are inspected at  $33.2^{\circ}\text{S}$  before they can interfere directly with the west coast upwelling system. In all other respects the Lagrangian calculations are numerically and virtually the same. We differentiate the new in-flight interception at  $33.2^{\circ}\text{S}$  according to the position with respect to the coastline, by grouping the particles that are over the shelf (limited by isobath 200 m), over the continental slope (limited by isobaths 200 and 1200 m) or further offshore (open ocean). Table 2 shows the partition of the transfer according to the final positions of the particles in the reference experiment (at  $12.7^{\circ}\text{E}$ , at  $30.45^{\circ}\text{S}$  or on the southern Benguela shelf) and their positions at  $33.2^{\circ}\text{S}$ . Less than 2% of Agulhas Bank waters that eventually reach the southern Benguela upwelling system (Table 2) are seen to travel at  $33.2^{\circ}\text{S}$  in the open ocean (0.01 Sv). Almost three-quarters of the transfer (0.27 Sv) follow a coastal route over the shelf and the



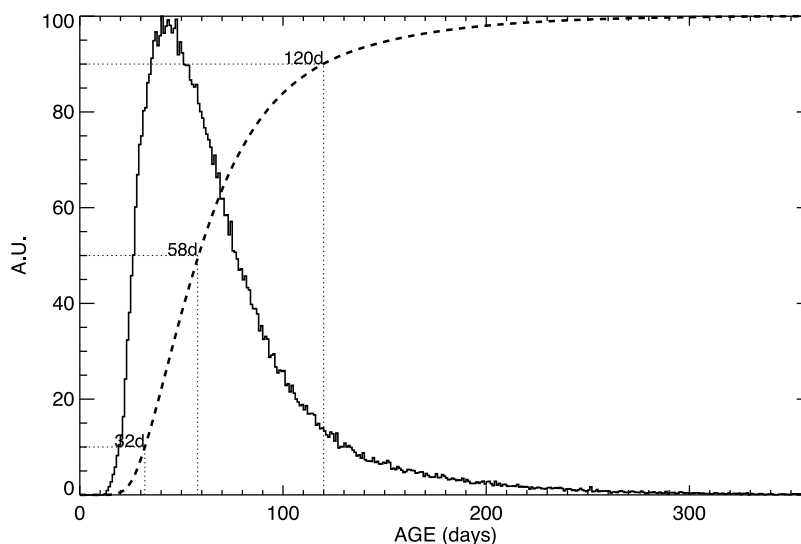


**Figure 8.** Histogram for the ages of the particles that participate in the mass transfer from the Agulhas Bank to the southern Benguela shelf, using 1 day bins. The thick dashed line shows the histogram integral whose asymptote is 100% of the mean transfer (i.e., 0.38 Sv) and is used to derive useful time scales such as the median transfer time (58 days).

remaining 25% (0.10 Sv) go northward through  $33.2^{\circ}\text{S}$  over the continental slope. However, a large fraction (78%) of the waters originating from the Agulhas Bank and in transit at  $33.2^{\circ}\text{S}$  over the continental slope (second column of Table 2) do not make their way to the west coast upwelling system, but eventually reach the more distant interception sections at  $30.45^{\circ}\text{S}$  (north) and  $12.7^{\circ}\text{E}$  (west) in equivalent proportions (0.17 Sv for each section). The situation for the waters in transit at  $33.2^{\circ}\text{S}$  over the shelf (third column of Table 2) is of course more in favor of a transmission to the west coast upwelling system (0.27 Sv), the transmission to  $30.45^{\circ}\text{S}$  and  $12.7^{\circ}\text{E}$  being only 0.05 and 0.03 Sv, respectively.

[18] We focus now on the time variability of the connection established between the Agulhas Bank and the continental slope and shelf at  $33.2^{\circ}\text{S}$  (slope and shelf in Table 2), restricting it to the waters that do not reach the southern Benguela upwelling system (0.42 Sv, by ignoring the southern Benguela shelf values in Table 2) and we compare it with that of the genuine transfer of water between the Agulhas Bank and the upwelling system. The flows contributing to the two transfers are referenced in Table 2 by 2 and 1, respectively, and are schematized in Figure 11. For each transfer, we construct a mean seasonal cycle both for the inflow on the Agulhas Bank (at locations  $A_2$  and  $A_1$ , see Figure 11) and for the intercepted flow at  $33.2^{\circ}\text{S}$  (at  $B_2$  and  $B_1$ ). For the connection we are studying in this paper, the linear correlation coefficient at  $33.2^{\circ}\text{S}$  (at location  $B_1$ ) between the time series of the flow itself and its mean seasonal cycle is now 0.74 (it was 0.79 when considered at its terminal stage on the edge of the southern Benguela shelf (at  $C_1$ ), and 0.61 when considered at its initial stage on the Agulhas Bank at location  $A_1$ ). For waters that follow the same initial path (over the slope and the shelf) but that are not to be captured by the west coast upwelling system, the equivalent correlation coefficients are only 0.33 and 0.36 at locations  $A_2$  and  $B_2$ , respectively.

Therefore, the seasonality of the connection established between the Agulhas Bank (at  $20.8^{\circ}\text{E}$ ) and  $33.2^{\circ}\text{S}$  depends on the fate of the waters north of that latitude. The transfer that is not captured by the west coast upwelling system is not associated with any significant seasonal signal over the Agulhas Bank while the genuine mass transfer from the Agulhas Bank to the southern Benguela upwelling system shows significant seasonal variability, inherent to seasonal variability in this coastal upwelling.

[19] Wind variability over the west coast is of course a major contributor to such variability, with its ability to drive seasonally the uplift of subsurface offshore water over the continental shelf. In this framework, the transfer of waters from the Agulhas Bank to the west coast upwelling system is seen as a seasonal draining among waters that flow almost continuously toward the subtropical Atlantic Ocean, within the Benguela Current, while keeping in mind that the surface wind stress is also able to move the waters away from the coast all along their journey, depending on the direction and intensity of its alongshore component. Figure 12 shows the alongshore component of the wind stress over the shelf of the west coast, during the full length of the simulation. The cross-shore component of the wind stress has a much smaller variability and a mean value close to 0 (not shown). The dynamical upwelling is active most of the year (with a mean value of the meridional wind stress equal to 0.032 Pa) but is maximum in summer (December–February) and minimum in June. Therefore, the peaks of variability of the wind stress coincide closely with the peaks of variability of the transfer when considered on the southern Benguela shelf. We note that the phase locking is not perfect, with the maximum of the wind stress occurring slightly after the maximum of the transfer (the time-lagged linear correlation coefficient of both time series is maximum for a 25 to 30 day lead time). This is because the surface wind stress is also active on the Agulhas Bank and drives a fraction of the westward flow (considered at

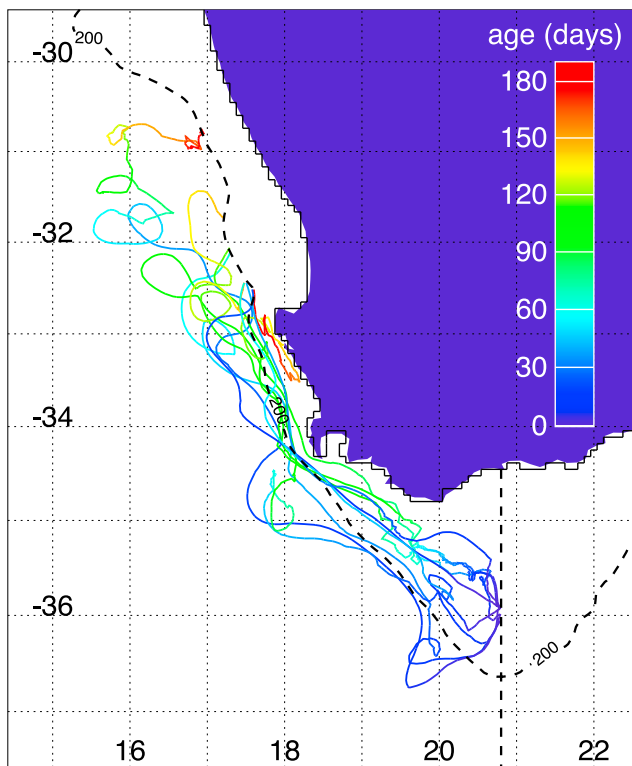


**Figure 9.** Selected set of nine individual trajectories that participate to the transfer of water from the Agulhas Bank and the southern Benguela shelf. Initial positions were chosen at  $20.8^{\circ}\text{E}$ , around  $36^{\circ}\text{S}$  ( $\pm 0.1^{\circ}$ ), and depth 20 m ( $\pm 2.5$  m), at the end of January ( $\pm 15$  days) over the full length of the simulation. The age of the particles is calculated since their point of departure at  $20.8^{\circ}\text{E}$  and is shown with a color code ranging from dark blue (0 days) to red (190 days, for the particle that presents the longest trajectory). Longitude  $20.8^{\circ}\text{E}$  and isobath 200 m, which defines the interception on the southern Benguela shelf, are drawn with thick dashed lines.

$20.8^{\circ}\text{E}$ ) away from the coastline (making it out of reach of the upwelling process on its arrival in the neighborhood of the west coast region). Wind variability over the Agulhas Bank indeed shows dominant episodes of southeasterlies in summer (Figure 13), at the same moment as the alongshore component of the wind stress is maximum in the southern Benguela upwelling system. On the Agulhas Bank, the offshore deflection by Ekman processes of the westward flow generates a fluctuation in the position of the coastal current at the westernmost edge of the bank (around  $18^{\circ}\text{E}$ ) that can interfere with the upwelling process on the west coast: it is not when upwelling winds blow their hardest on the west coast that  $20.8^{\circ}\text{E}$ -originating waters are the most likely to be present at the entrance of the upwelling cell. For other seasons, the alongshore component of the wind on the Agulhas Bank turns eastward and cannot drive the westward oceanic flow away from the coastline. In accordance with this seasonal cycle on the wind stress, the coastal upwelling jet is only present in spring and summer, decreasing through autumn and is not apparent in winter [Chang, 2009].

#### 4.2. Intraseasonal Events

[20] In addition to seasonal variability, the transfer of waters from the Agulhas Bank to the west coast upwelling shows irregularity on intraseasonal scales (Figure 14). Such anomalies can appear as monthlong periods over which the modeled transfer, averaged over 10 day bins, is consistently smaller (such as in late 1997, mid-1999, and mid-2003) or larger (such as in early 1998, mid-1999, and early 2004) than its mean seasonal value. The anomalies translate in interannual contrasts when computing for each year of the simulation the volume of water transferred from the Agulhas Bank to the southern Benguela shelf. Such annual transfers can vary by as much as 80% from year to year, with extreme values of 0.28 and 0.51 Sv in 1997 and 1998, respectively. Time series of intraseasonal anomalies calculated at the two ends of the transfer (i.e., for the inflow on the Agulhas Bank at  $20.8^{\circ}\text{E}$  and for the outflow on the southern Benguela shelf) over 10 day time intervals still present a maximum cross-correlation coefficient (0.60) for a 40 day lag (the coefficient was 0.74 when seasonal variability was included; see section 4.1). Intraseasonal anomalies apparent at both ends of the transfer are thus related. It is not only a question of local and temporary modulation of the strength of the inflow and outflow time series. Moreover, such events are not associated with specific wind events along the path of the connection, as noticeable on the time series of the wind stress (Figure 12) and of the transfer (Figure 10) and evidenced by very poor cross-correlation coefficients (less than 0.1) between outflow or inflow intraseasonal anomalies and wind stress anomalies, whatever the value chosen for the time lag.

[21] The ocean around southern Africa and more especially along the Benguela Current is characterized by internal variability, which can generate interannual sea surface temperature anomalies over the shelf along the western coast [Blanke *et al.*, 2002], but also change the main features of the connection established between the Agulhas Bank and the west coast upwelling system and possibly disrupt it or intensify it momentarily. Irregularity in the way the Agulhas Current rushes down along the Agulhas Bank is here the main reason for such intraseasonal variability. Figure 15 shows maps of the modeled sea level for selected moments when the connection under study almost vanishes or significantly increases. The presence of cyclonic activity to the southwest and south-southwest of the Agulhas Bank is synonymous with a deflection of the Agulhas flow away from the western side of the Agulhas Bank. On the contrary, anticyclonic eddies in the same place appear very effective for channeling northwestward along and over the shelf a significant fraction of the Agulhas flow that will eventually turn around the southwestern corner of Africa and reach the west coast upwelling system. In the former configuration, the particles used in our Lagrangian experiment are prone to a southward export to the interception section located at  $37.5^{\circ}\text{S}$ . In the latter case, they are freer to move along the Agulhas Bank, avoiding this early interception. As a more synthetic index, we calculate the integral of surface relative vorticity over a domain that extends from  $16$  to  $21^{\circ}\text{E}$  and from  $35$  to  $38^{\circ}\text{S}$  and over bottom topography deeper than 1200 m. The index is shown as 10 day averages on Figure 16 for the period of the simulation when substantial intraseasonal anomalies (i.e.,

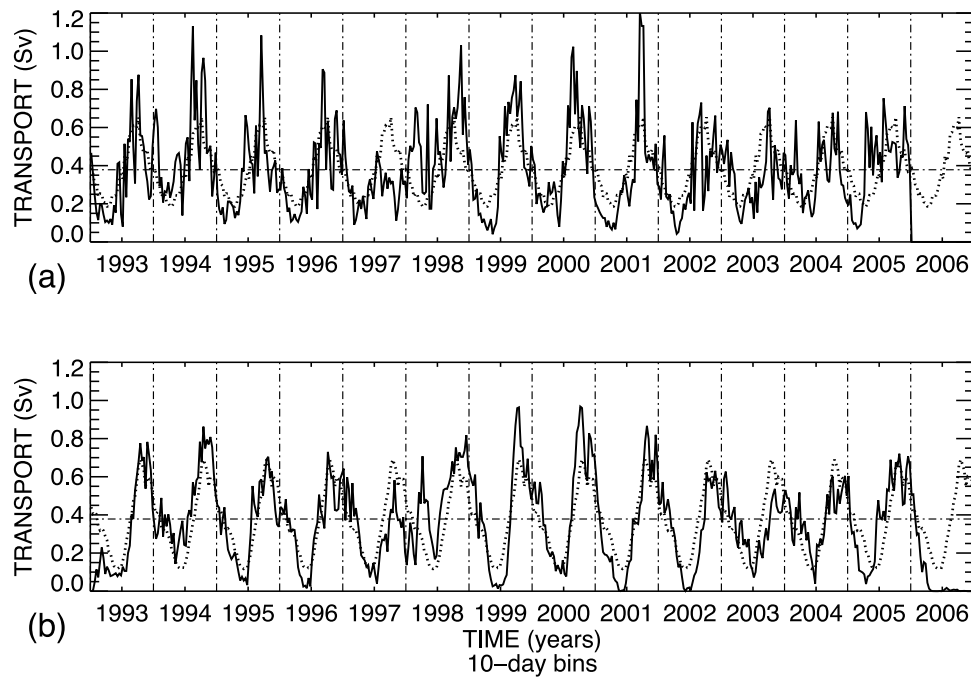


**Figure 10.** Time variability of the mass transfer achieved in the model from the Agulhas Bank to the southern Benguela shelf (a) for the inflow at  $20.8^{\circ}\text{E}$  and (b) upon arrival in the west coast upwelling system. Mean seasonal cycles are calculated over the 1994–2005 period and are superimposed with thick dotted lines. The mean value of the transfer (0.38 Sv) is indicated by horizontal lines.

larger than 0.1 Sv for more than 7 successive weeks) were found to occur in the volume transfer from the Agulhas Bank to the southern Benguela upwelling system (1997–2000 and 2003–2004; see Figures 14a and 15). The agreement between both curves is fair with intensified connection obtained for the largest positive values of the integrated vorticity index (predominance of anticyclonic conditions) and, conversely, reduction in transport for cyclonic conditions. The phasing of both time series is however not perfect over the full 1994–2005 time series, which suggests the importance of other physical processes in setting up perturbations of smaller amplitude in the transferred flow to the west coast. Such processes of course include local air-sea interactions (particularly short-lived wind stress events) and irregularities in the Agulhas flow that rushes down the southeastern coast of Africa. Such intraseasonal and interannual anomalies have likely an impact on biology as stated for instance by *Olyott et al.* [2007] for the chokka squid.

## 5. Discussion and Concluding Remarks

[22] *Blanke et al.* [2005] showed by looking at the vertical structure of the onshore and offshore currents that the southernmost area of the southern Benguela upwelling region is mostly associated with coastward movements, whereas the circulation further north shows a clearer contrast between surface-expelled and subsurface-upwelled waters. This difference fits the view of a mean flow and mesoscale structures transmitted northward from the retro-reflection area of the Agulhas Current together with the Benguela Current, flowing up the continental slope in its southernmost portion (see Figure 4) and interacting with the

upwelling circulation before attenuation over the shelf and export by Ekman divergence.

[23] This study used the physical fields issued from a high-resolution ocean general circulation model to investigate the nature and variability of the connection established between the Agulhas Bank (considered at  $20.8^{\circ}\text{E}$ ) and the southern Benguela continental shelf (chosen in this study as the area from the coast to the 200 m isobath). Our results rest on the interpretation of millions of Lagrangian particles, in a way somewhat similar to the one followed by *Huggett et al.* [2003] for studying the transport success of anchovy eggs and larvae in the southern Benguela upwelling system. The strength of our approach is the use of the ARIANE toolkit for calculating trajectories in the three-dimensional, time-varying, model velocity output. It allows volume transport estimates on the basis of the infinitesimal weight allotted to each particle and carried along its trajectory. The transfer of water from the Agulhas Bank to the southern

**Table 2.** Crossed Analysis of the Results of the Reference Lagrangian Experiment and Test Lagrangian Experiment<sup>a</sup>

Final Interception in the Reference Experiment	In-Flight Interception at $33.2^{\circ}\text{S}$ (Sv)		
	Open Ocean	Slope	Shelf
West at $12.7^{\circ}\text{E}$	0.33 (3)	0.17 (2)	0.03 (2)
North at $30.45^{\circ}\text{S}$	0.12 (3)	0.17 (2)	0.05 (2)
Southern Benguela shelf	0.01	0.10 (1)	0.27 (1)

<sup>a</sup>With, notably, two interception sections located at the edge of the Benguela shelf and at  $30.45^{\circ}\text{S}$ . Here the former sections are replaced by a unique section at  $33.2^{\circ}\text{S}$ , with differentiation of the shelf, slope, and open ocean domains, for which the model ocean floor is shallower than 200 m, between 200 and 1200 m, and deeper than 1200 m, respectively. Numbers in parentheses identify the transfers that are sketched in Figure 11.

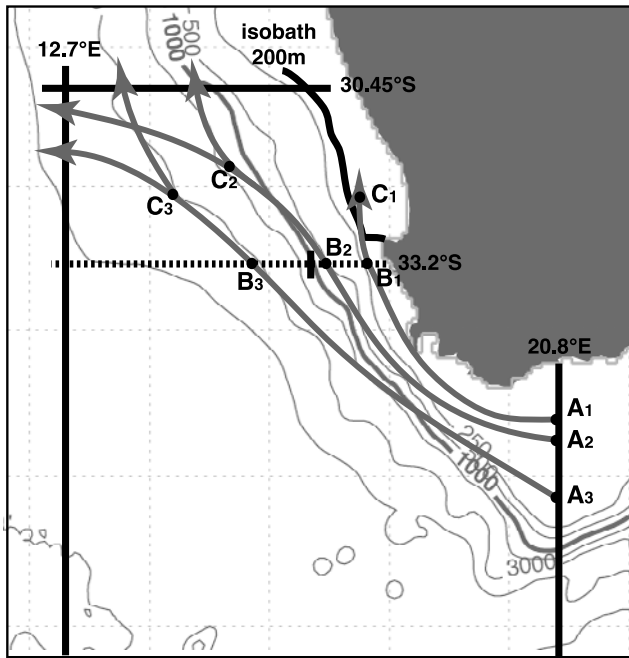


**Figure 11.** Schematic view of the main volume transfers achieved from 20.8°E (on the Agulhas Bank) to the edge of the southern Benguela shelf and to the subtropical Atlantic (at 12.7°E or 30.45°S, see Figure 4). Transfer A<sub>1</sub>-B<sub>1</sub>-C<sub>1</sub> (denoted by 1 in Table 2) shows the connection established between the Agulhas Bank and the southern Benguela upwelling system; it flows almost entirely over the continental slope and shelf (i.e., over depths shallower than 1000 m) at 33.2°S. Transfer A<sub>2</sub>-B<sub>2</sub>-C<sub>2</sub> (denoted by 2 in Table 2) shows the Agulhas Bank waters exported to 12.7°E or 30.45°S that also flow over the continental slope and shelf at 33.2°S. Transfer A<sub>3</sub>-B<sub>3</sub>-C<sub>3</sub> (denoted by 3 in Table 2) is the remaining export of Agulhas Bank waters to 12.7°E and 30.45°S, with a passage at 33.2°S over the deep ocean (offshore the continental slope). The seasonal variability of the first two transfers is discussed in the text.

Benguela upwelling system can be construed as the displacement of fluid across a rubber balloon pierced at its both ends. The fluid enters one end of the balloon with some specific time variability, and exits at the other end with a modified variability. The elasticity of the balloon accounts

for local dilatation or contraction equivalent to local accumulation or withdrawal of fluid: the advective transport of fluid is not uniform across the balloon. We could assess the magnitude of the connection actually achieved between two end sections and the variability of the transfer, conveniently expressed in sverdrups, could be investigated on different time scales. As the initial section was chosen in the middle or the Agulhas Bank, our results bear some relation with the transport success of anchovy eggs calculated by *Huggett et al.* [2003] from several subregions over the Agulhas Bank to the nursery area in the southern Benguela upwelling system. One must keep in mind, however, that in addition to the ocean modeling framework itself, our Lagrangian approach somewhat differs from the particle-tracking strategy adopted by *Huggett et al.* [2003]. Among other differences, our initialization strategy aims at optimizing the distribution of particles all over a meridional section by grouping them where the incoming transport is the largest (so that their individual weight is comparable), whereas *Huggett et al.* [2003] favor a random vertical distribution, furthermore limited to the upper 60 m of the ocean, within a given horizontal patchiness over several subregions of the Agulhas Bank. Moreover, their tracking period is limited to 60 days, a value compatible with the expected duration of eggs and larvae development, while we integrate Lagrangian trajectories up to 1 year to account for most time scales of the water mass transfer under study. Despite these practical differences, the mean seasonal cycle we obtain for the magnitude of the Lagrangian connection matches very well the transport success diagnosed by *Huggett et al.* [2003] in relation to the month of spawning on the Agulhas Bank, with the lowest and largest values obtained in May–July and October–January, respectively. However, our interpretation of this seasonal variability is different. From a pure physical point of view, in the model simulation, oceanic conditions on the Agulhas Bank cannot be put forward as a main explanation of the variability of the transfer. In our study, indeed, the conditioning parameters are to be found downstream and are closely linked to the variability of the alongshore component of the wind stress that drives in particular the seasonal variability of the upwelling system on the west coast. Over the Agulhas Bank, no clear seasonal signal exists in the full westward flow at 20.8°E. Only the fraction of this flow that will eventually reach the southern Benguela upwelling system is associated with significant

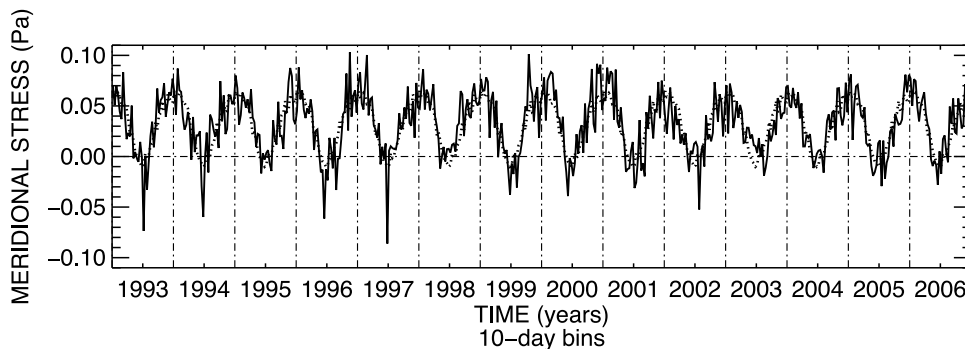


**Figure 12.** Time variability on the southern Benguela shelf (at 17°E, 32°S) of the alongshore component of the NCEP wind stress that was used to force the model. The mean seasonal cycle calculated over 1994–2005 is repeated as a thick dotted line.

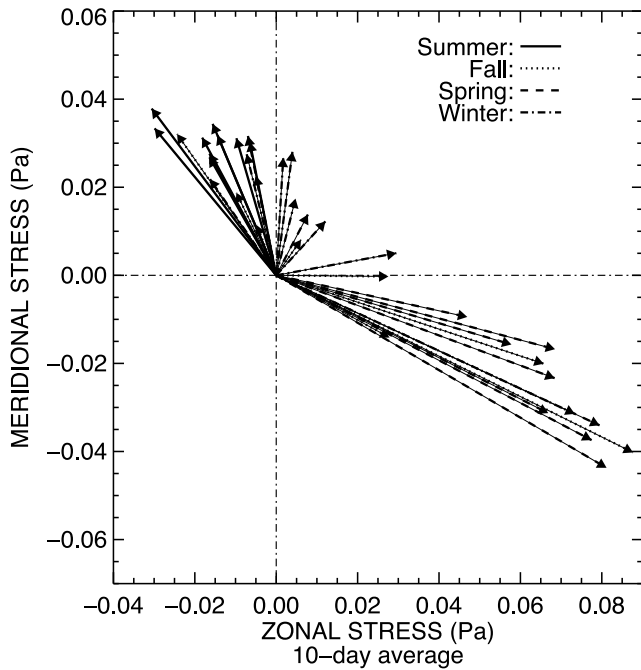


**Figure 13.** Mean seasonal variability on the Agulhas Bank (at 20°E, 35.5°S) of the NCEP wind stress that was used to force the model. Each arrow corresponds to a 10 day period and arrow line styles differ according to the season.

seasonal variability. The flow of water that originates from the Agulhas Bank at 20.8°E, moves over the shelf or near the slope till 32°S without being captured by the west coast continental shelf does not show seasonal variability.

[24] The simulation we analyze in this study includes both intraseasonal and interannual variability, introduced at the sea surface by the wind stress and at the lateral open boundary conditions by information from the parent grid or produced internally by the ocean. Among other improvements, the SAfE approach [Penven *et al.*, 2006a, 2006b] we use in this new study allows better coupling of the coastal dynamics with the surrounding large-scale ocean dynamics (using the AGRIF system), better representation of meso-scale features thanks to a slightly higher spatial resolution, and genuine account for interannual surface wind stress variability (as present in the NCEP reanalysis). The SAfE modeling approach has been shown to produce realistic and potent results for the study of various marine ecosystems along the coast of southern Africa [Penven *et al.*, 2006a, 2006b; Veitch *et al.*, 2009]. Within this framework, large intraseasonal anomalies diagnosed in the transfer of water from the Agulhas Bank to the southern Benguela upwelling system find their origin mostly in the presence and movement of mesoscale structures along the western edge of the Agulhas Bank. The generation and evolution of the eddy field southwest of Africa is of course very chaotic and is appropriately rendered by the “Cape Cauldron” appellation introduced by Boebel *et al.* [2003]. It is partly dependent on the way the Agulhas Current retroflects into the Indian

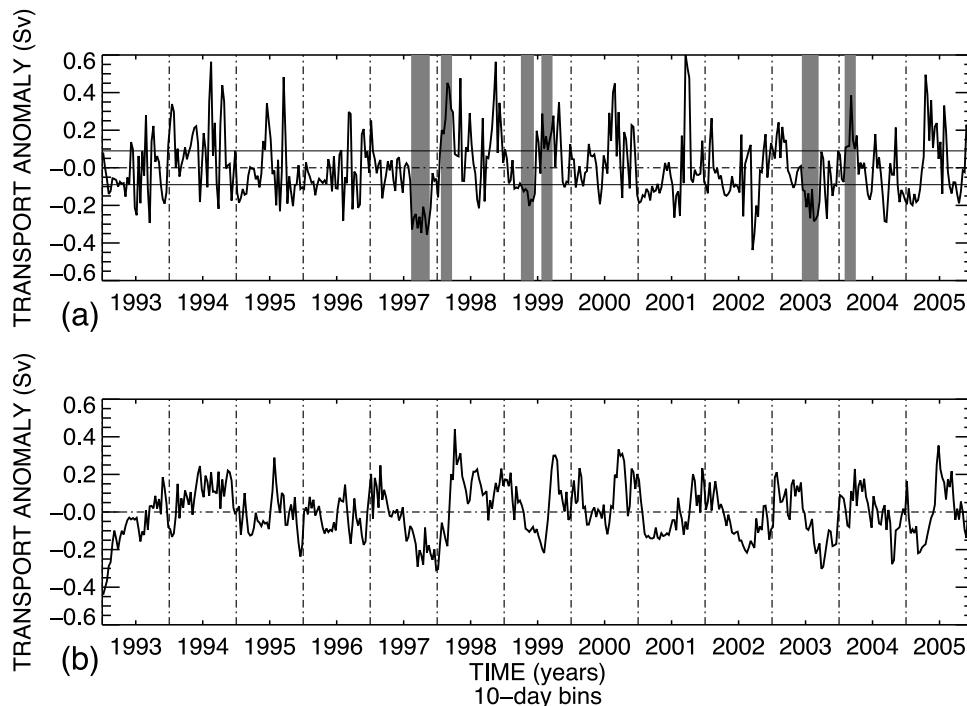


**Figure 14.** Interannual variability of the mass transfer from the Agulhas Bank to the southern Benguela shelf (a) for the inflow at 20.8°E and (b) upon arrival in the west coast upwelling system. The raw time series of the transfer and the mean seasonal cycles shown in Figure 10 were used for the calculation of the anomalies. Selected moments corresponding to pronounced transport anomalies (larger than 0.1 Sv for more than 7 successive weeks) are shaded and discussed in section 4.2.

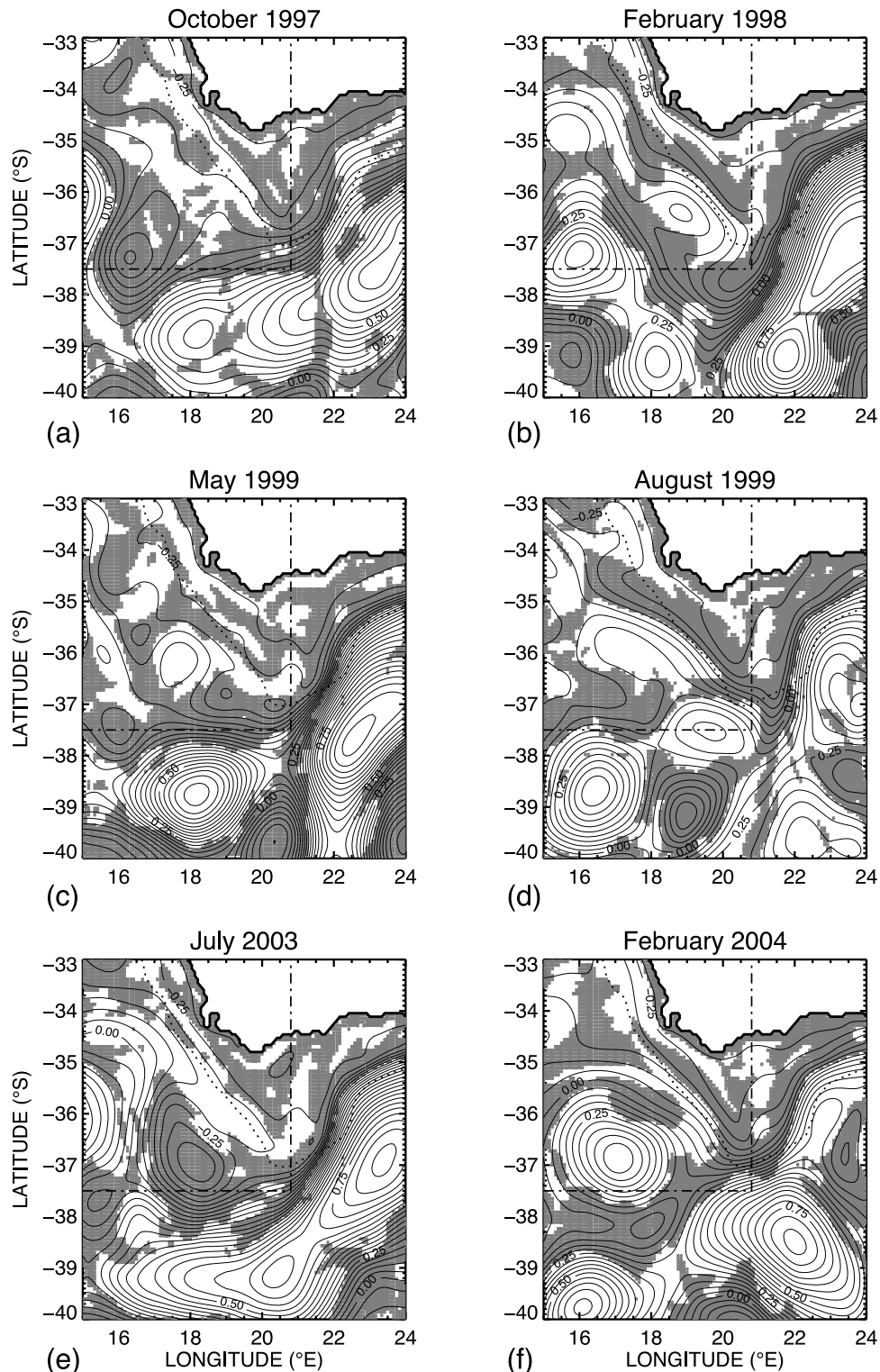


**Figure 15.** Sea level maps for selected periods of the model simulation corresponding to significant negative (on the left-hand side) and positive (on the right-hand side) anomalies in the variability of the mass transfer from the Agulhas Bank to the southern Benguela shelf (see Figure 14). The contour interval is 0.05 m. The domain of integration of the Lagrangian experiment and the isobath 1200 m are shown with a dot-dashed and dotted line, respectively. Shaded areas show regions where the Laplacian of the sea level (an equivalent of the opposite of relative vorticity of the surface absolute geostrophic circulation in the Southern Hemisphere) is positive, a good index of near surface cyclonic circulation.

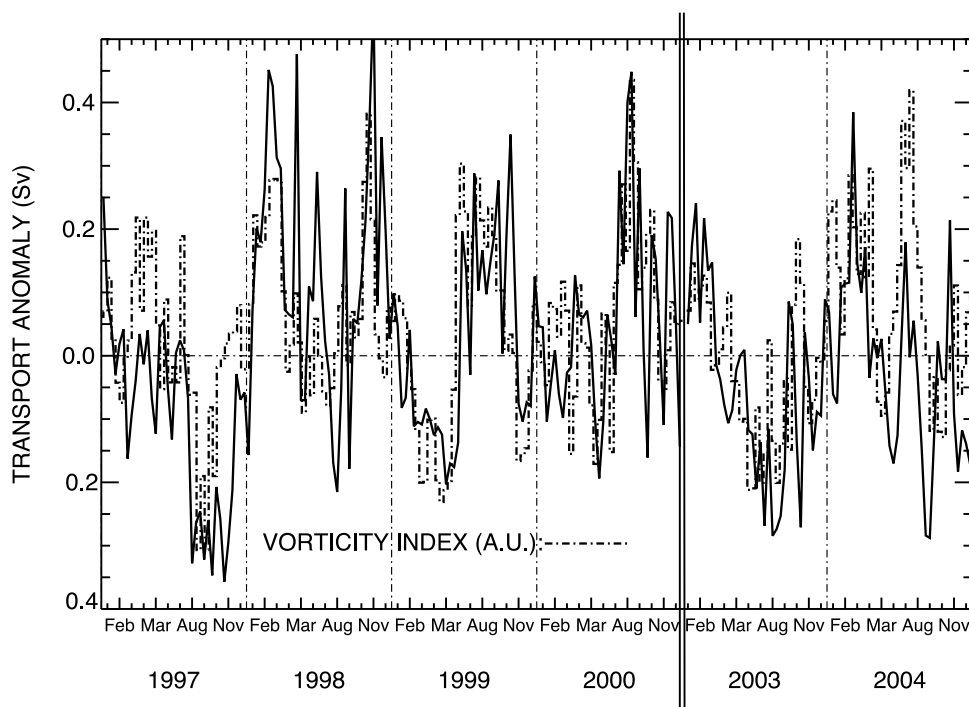


**Figure 16.** Interannual variability of the mass transfer from the Agulhas Bank to the southern Benguela shelf over 1997–2000 and 2003–2004 (thick curve, see Figure 14a) and surface relative vorticity integrated over the region  $[16^{\circ}\text{E}–21^{\circ}\text{E}] \times [38^{\circ}\text{S}–35^{\circ}\text{S}]$  with bottom topography deeper than 1200 m off the southwest edge of the Agulhas Bank (dashed histogram, arbitrary unit).

Ocean, and on the deepness of its penetration in the Atlantic Ocean. Upstream variability, possibly induced by Natal pulses or shear edge features with origins as remote as the Mozambique Channel, may also trigger the behavior of the Agulhas Current south of the Agulhas Bank [van Leeuwen *et al.*, 2000; Penven *et al.*, 2006a; Quartly *et al.*, 2006], making its dynamics somewhat unpredictable. Then, though our study could not associate intraseasonal variability in mass transfer with specific wind events, one must keep in mind that regional ocean modeling could still benefit from improved atmospheric forcing fields. Near real time blended surface winds, for which remotely sensed wind retrievals are blended with operational wind analyses (issued from meteorological models), aim at providing such enhanced spatial and temporal resolution [e.g., Bentamy *et al.*, 2006]. Therefore, one of our first priorities would be to lead this study with such improved winds. Future numerical work also aims at running sensitivity experiments, in which some physical processes can be switched off or on (such as upstream variability in the Agulhas Current). Indeed, our study does not succeed to deconvolute fully the contributions of the wind stress and of eddy variability to the variability of the transfer of water from the Agulhas Bank to the southern Benguela upwelling system, even though it identifies the main contributors to the seasonal variability of the transfer (the wind) and to large intraseasonal events (eddy activity).

[25] The return journey of anchovy recruits to the Agulhas Bank spawning ground cannot be addressed with a physical model alone. Anchovy behavior, swimming ability and food availability are some biological keys [e.g., Griffiths *et al.*, 2004] that are ignored in our framework. Though we

could investigate a preferential pathway, imposed uniquely by the existence of a southeastward flowing vein of current around southern Africa from the southern edge of the west coast upwelling system to the Agulhas Bank, anchovy mobility rates as well as survival rates constitute essential ingredients for a thorough investigation. End-to-end modeling that integrates biological and physical processes at different scales and two-way interactions between several ecosystem components is a promising way to achieve such ends [Travers *et al.*, 2007], knowing that high-resolution physical modeling remains one essential constituent of these complex tools.

[26] **Acknowledgments.** We thank two anonymous reviewers and the editor for helpful and detailed comments. Support for this study has been provided by the Centre National de la Recherche Scientifique (CNRS) for B.B. and by the Institut de Recherche pour le Développement for P.P. and C.R. This study is also a contribution to InterUp, a project funded by the French LEFE-IDAO program (Les Enveloppes Fluides et l'Environnement-Interactions et Dynamique de l'Atmosphère et de l'Océan). Numerical simulations were performed with the computational resources available at LPO and at the Centre de Brest of IFREMER.

## References

- Bang, N. D., and W. R. H. Andrews (1974), Direct current measurements of a shelf-edge frontal jet in the southern Benguela system, *J. Mar. Res.*, *32*, 405–417.
- Bentamy, A., H.-L. Ayina, P. Queffelec, and D. Croize-Fillon (2006), Improved near real time surface wind resolution over the Mediterranean Sea, *Ocean Sci. Discuss.*, *3*, 435–470.
- Blanke, B., and S. Raynaud (1997), Kinematics of the Pacific Equatorial Undercurrent: An Eulerian and Lagrangian approach from GCM results, *J. Phys. Oceanogr.*, *27*, 1038–1053, doi:10.1175/1520-0485(1997)027<1038:KOTPEU>2.0.CO;2.
- Blanke, B., M. Arhan, G. Madec, and S. Roche (1999), Warm water paths in the equatorial Atlantic as diagnosed with a general circulation model,

- J. Phys. Oceanogr.*, 29, 2753–2768, doi:10.1175/1520-0485(1999)029<2753:WWPITE>2.0.CO;2.
- Blanke, B., C. Roy, P. Penven, S. Speich, J. Mc Williams, and G. Nelson (2002), Linking wind and upwelling interannual variability in a regional model of the southern Benguela, *Geophys. Res. Lett.*, 29(24), 2188, doi:10.1029/2002GL015718.
- Blanke, B., S. Speich, A. Bentamy, C. Roy, and B. Sow (2005), Southern Benguela upwelling and QuikSCAT wind variability, *J. Geophys. Res.*, 110, C07018, doi:10.1029/2004JC002529.
- Blayo, E., and L. Debreu (1999), Adaptive mesh refinement for finite difference ocean model: Some first experiments, *J. Phys. Oceanogr.*, 29, 1239–1250, doi:10.1175/1520-0485(1999)029<1239:AMRFFD>2.0.CO;2.
- Boebel, O., J. Lutjeharms, C. Schmid, W. Zenk, T. Rossby, and C. Barron (2003), The cape cauldron: A regime of turbulent inter-ocean exchange, *Deep Sea Res. Part II*, 50, 57–86, doi:10.1016/S0967-0645(02)00379-X.
- Chang, N. (2009), Numerical ocean model study of the Agulhas Bank and the Cool Ridge, Ph.D. thesis, 182 pp., Univ. of Cape Town, Cape Town, South Africa.
- Conkright, M. E., R. Locarnini, H. Garcia, T. O'Brien, T. P. Boyer, C. Stephens, and J. Antonov (2002), World Ocean Atlas 2001: Objective analyses, data statistics, and figures, CD-ROM documentation, *Internal Rep. 17*, Natl. Oceanogr. Data Cent., Silver Spring, Md.
- Ducet, N., P.-Y. Le Traon, and G. Reverdin (2000), Global high-resolution mapping of ocean circulation from TOPEX/Poseidon and ERS-1 and -2, *J. Geophys. Res.*, 105(C8), 19,477–19,498, doi:10.1029/2000JC900063.
- Griffiths, C. L., et al. (2004), Impacts of human activities on marine life in the Benguela: A historical overview, *Oceanogr. Mar. Biol.*, 42, 303–392.
- Hardman-Mountford, N. J., A. J. Richardson, J. J. Agenbag, E. Hagen, L. Nykjaer, F. A. Shillington, and C. Villacastin (2003), Ocean climate of the south east Atlantic observed from satellite data and wind models, *Prog. Oceanogr.*, 59, 181–221, doi:10.1016/j.pocean.2003.10.001.
- Hodur, R. M. (1997), The Naval Research Laboratory's Coupled Ocean/Atmosphere Mesoscale Prediction System (COAMPS), *Mon. Weather Rev.*, 125, 1414–1430, doi:10.1175/1520-0493(1997)125<1414:TNRWSC>2.0.CO;2.
- Huggett, J., P. Freon, C. Mullan, and P. Penven (2003), Modelling the transport success of anchovy *Engraulis encrasicolus* eggs and larvae in the southern Benguela: The effect of spatio-temporal spawning patterns, *Mar. Ecol. Prog. Ser.*, 250, 247–262, doi:10.3354/meps250247.
- Hutchings, L. (1992), Fish harvesting in a variable, productive environment - searching for rules of searching for exceptions?, *S. Afr. J. Mar. Sci.*, 12, 297–318.
- Lutjeharms, J. R. E., R. Catzel, and H. R. Valentine (1989), Eddies and other border phenomena of the Agulhas Current, *Cont. Shelf Res.*, 9, 597–616, doi:10.1016/0278-4343(89)90032-0.
- Olyott, L. J. H., W. H. H. Sauer, and A. J. Booth (2007), Spatial patterns in the biology of the chokka squid, *Loligo reynaudii* on the Agulhas Bank, South Africa, *Rev. Fish Biol. Fish.*, 17, 159–172, doi:10.1007/s11160-006-9027-5.
- Penven, P., J. R. E. Lutjeharms, and P. Florenchie (2006a), Madagascar: A pacemaker for the Agulhas Current system?, *Geophys. Res. Lett.*, 33, L17609, doi:10.1029/2006GL026854.
- Penven, P., N. Chang, and F. Shillington (2006b), Modelling the Agulhas Current using SAfE (Southern Africa Experiment), *Geophys. Res. Abstr.*, 8, abstract 04225.
- Penven, P., L. Debreu, P. Marchesiello, J. C. McWilliams, and A. F. Shchepetkin (2006c), Application of the ROMS embedding procedure to the central California upwelling system, *Ocean Modell.*, 12, 157–187, doi:10.1016/j.ocemod.2005.05.002.
- Penven, P., P. Marchesiello, L. Debreu, and J. Lefèvre (2007), Software tools for pre- and post-processing of oceanic regional simulations, *Environ. Model. Softw.*, 23, 660–662, doi:10.1016/j.envsoft.2007.07.004.
- Quarty, G. D., J. J. H. Buck, M. A. Srokosz, and A. C. Coward (2006), Eddies around Madagascar: The retroflexion re-considered, *J. Mar. Syst.*, 63, 115–129, doi:10.1016/j.jmarsys.2006.06.001.
- Rio, M.-H., and F. Hernandez (2004), A mean dynamic topography computed over the world ocean from altimetry, in situ measurements, and a geoid model, *J. Geophys. Res.*, 109, C12032, doi:10.1029/2003JC002226.
- Shchepetkin, A. F., and J. C. McWilliams (2005), The regional oceanic modeling system (ROMS): A split-explicit, free-surface, topography-following-coordinate oceanic model, *Ocean Modell.*, 9, 347–404, doi:10.1016/j.ocemod.2004.08.002.
- Shelton, P. A., and L. Hutchings (1982), Transport of anchovy, *Engraulis capensis* Gilchrist, eggs and early larvae by a frontal jet current, *J. Cons. Cons. Int. Explor. Mer.*, 40, 185–198.
- Shillington, F. A., C. J. C. Reason, C. M. Duncombe Rae, P. Florenchie, and P. Penven (2006), Large scale physical variability of the Benguela Current Large Marine Ecosystem (BCLME), in *Benguela: Predicting a Large Marine Ecosystem*, edited by V. Shannon et al., pp. 49–70, Elsevier, Amsterdam.
- Travers, M., Y.-J. Shin, S. Jennings, and P. Cury (2007), Towards end-to-end models for investigating the effects of climate and fishing in marine ecosystems, *Prog. Oceanogr.*, 75, 751–770, doi:10.1016/j.pocean.2007.08.001.
- van der Lingen, C. D., J. C. Coetzee, and L. Hutchings (2002), Temporal shifts in the spatial distribution of anchovy spawners and their eggs in the southern Benguela: Implications for recruitment, in *Report of a GLOBEC-SPACC/IDYLE/ENVIFISH Workshop on Spatial Approaches to the Dynamics of Coastal Pelagic Resources and Their Environment in Upwelling Areas*, edited by C. D. van der Lingen et al., pp. 46–48, Global Ocean Ecosyst. Dyn. Int. Proj. Off., Plymouth, U. K.
- van Leeuwen, P. J., W. P. M. de Ruijter, and J. R. E. Lutjeharms (2000), Natal pulses and the formation of Agulhas Rings, *J. Geophys. Res.*, 105(C3), 6425–6436, doi:10.1029/1999JC900196.
- Veitch, J., P. Penven, and F. Shillington (2009), The Benguela: A laboratory for comparative modelling studies, *Prog. Oceanogr.*, doi:10.1016/j.pocean.2009.07.008, in press.
- Weeks, S. J., R. Barlow, C. Roy, and F. A. Shillington (2006), Remotely sensed variability of temperature and chlorophyll in the southern Benguela: Upwelling frequency and phytoplankton response, *Afr. J. Mar. Sci.*, 28, 493–509.

B. Blanke, Laboratoire de Physique des Océans, UMR 6523, UBO, CNRS, IRD, IFREMER, 6 Ave. Le Gorgeu, F-29238 Brest CEDEX 3, France. (blanke@univ-brest.fr)

N. Chang, Center for High Performance Computing, CSIR, CSIR Campus, 15 Lower Hope St., Rosebank, Cape Town 7700, South Africa. (nchang@csir.co.za)

F. Kokoszka, P. Penven, and C. Roy, Laboratoire de Physique des Océans, UMR 6523, UBO, IRD, CNRS, IFREMER, Centre IFREMER de Brest, BP 70, F-29280 Plouzané, France. (florian.kokoszka@ifremer.fr; pierrick.penven@ird.fr; claude.roy@ird.fr)